Vitrimers

International Edition: DOI: 10.1002/anie.201912223
German Edition: DOI: 10.1002/ange.201912223

Conformational Entropy as a Means to Control the Behavior of Poly(diketoenamine) Vitrimers In and Out of Equilibrium

Changfei He, Peter R. Christensen, Trevor J. Seguin, Eric A. Dailing, Brandon M. Wood, Rebecca K. Walde, Kristin A. Persson, Thomas P. Russell, and Brett A. Helms**

Abstract: *Control of equilibrium and non-equilibrium thermomechanical behavior of poly(diketoenamine) vitrimers is shown by incorporating linear polymer segments varying in molecular weight (MW) and conformational degrees of freedom into the dynamic covalent network. While increasing MW of linear segments yields a lower storage modulus at the rubbery plateau after softening above the glass transition (T_g), both T_g and the characteristic time of stress relaxation are independently governed by the conformational entropy of the embodied linear segments. Activation energies for bond exchange in the solid state are lower for networks incorporating flexible chains; the network topology freezing temperature decreases with increasing MW of flexible linear segments but increases with increasing MW of stiff segments. Vitrimer reconfigurability is therefore influenced not only by the energetics of bond exchange for a given network density, but also the entropy of polymer chains within the network.*

Vitrimers are living polymer networks that reconfigure via dynamic associative bond-exchange reactions, laying the foundations for both self-healing plastics and post-industrial plastics recycling.[1–3] The cross-linking density of a vitrimer influences its thermal and mechanical properties: for example, higher network density increases the probability that cross-links will interact and be involved in bond-exchange reactions, which impact the dynamics of vitrimer reconfigurability across multiple length scales and therefore its rheology. The energetics of bond-exchange reactions have been studied for vitrimers undergoing uncatalyzed or catalyzed transesterification,[4–6] transcarbamoylation,[7–10] olefin metathesis,[11] boronic ester exchange,[12–14] siloxane exchange,[15,16] triazolium transalkylation,[17] imine bond exchange,[18,19] ketoenamine exchange,[20–22] and diketoenamine exchange.[23] However, there is a lack of understanding of how conformational degrees of freedom available to the network influence a vitrimer's thermal and rheological behavior in and out of equilibrium. Understanding these aspects is key to establishing guidelines for vitrimer processing.

Herein, we show that the incorporation of conformationally flexible or, alternatively, stiff ditopic (A2) monomers into a vitrimer network otherwise comprised of tritopic (A3) and ditopic B2 monomers allows the network density to be independently modulated from the thermal, mechanical, and rheological properties of the network. We exerted fine-control over such architectural attributes in a vitrimer using poly(diketoenamine)s, or PDKs, which click together via spontaneous condensation reactions between polytopic triketone and amine monomers (Figure 1a).[23] PDK **1**, which exhibits the highest network density, was generated from ditopic triketone monomer TK-10 and tris(aminoethyl)amine (TREN) as the crosslinker. We also introduced to PDK **1** linear segments of varying molecular weight with conformational degrees of freedom by adding either trimethylhexamethylene diamine (TMHDA) or isophorone diamine (IPDA) in controlled amounts (20–60 mol%) to the reaction mixture (Figure 1c). Torsional partition functions, q_{tor}, for TMHDA- and IPDA-based monomer segments differentiate each monomer by conformational degrees of freedom; by extension, linear PDK segments incorporating TMHDA and IPDA are comparably flexible or stiff, respectively (Figure 1b). THMDA, IPDA, and dimedone-derived TK monomers each originate from acetone as a common starting

[*] C. He, Prof. Dr. T. P. Russell
Beijing Advanced Innovation Center
for Soft Matter Science and Engineering Beijing University
of Chemical Technology
Beijing 100029 (China)
E-mail: tom.p.russell@gmail.com

Dr. P. R. Christensen, Dr. E. A. Dailing, R. K. Walde, Dr. B. A. Helms
The Molecular Foundry,
Lawrence Berkeley National Laboratory
1 Cyclotron Road, Berkeley, CA 94720 (USA)
E-mail: bahelms@lbl.gov

Dr. T. J. Seguin
Energy Technologies Area,
Lawrence Berkeley National Laboratory
1 Cyclotron Road, Berkeley, CA 94720 (USA)

B. M. Wood
Graduate Group of Applied Science and Technology
University of California, Berkeley, CA 94720 (USA),
and
Environmental Energy Technologies Division
Lawrence Berkeley National Laboratory
1 Cyclotron Road, Berkeley, CA 94720 (USA)

Prof. Dr. K. A. Persson
Materials Science and Engineering Department
University of California, Berkeley, CA 94720 (USA)

Prof. Dr. T. P. Russell, Dr. B. A. Helms
Materials Sciences Division,
Lawrence Berkeley National Laboratory
1 Cyclotron Road, Berkeley, CA 94720 (USA)

Prof. Dr. T. P. Russell
Polymer Science and Engineering Department
University of Massachusetts
Amherst, MA 01003 (USA)

Supporting information and the ORCID identification number(s) for the author(s) of this article can be found under: https://doi.org/10.1002/anie.201912223.

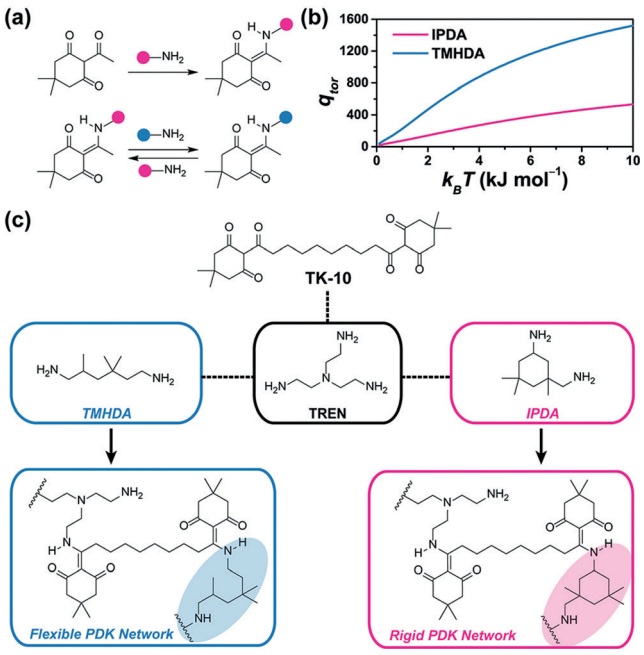

Figure 1. a) Triketones and amines self-condense to yield dynamic covalent diketoenamines, which undergo bond exchange reactions with amines. b) Torsional partition functions, q_{tor}, differentiating the conformational degrees of freedom for TMHDA- and IPDA-based small molecule models of the microstructural elements in PDK vitrimers **2**–**7**. c) Synthesis of PDK vitrimers **1**–**7** via clickable polycondensation reactions.

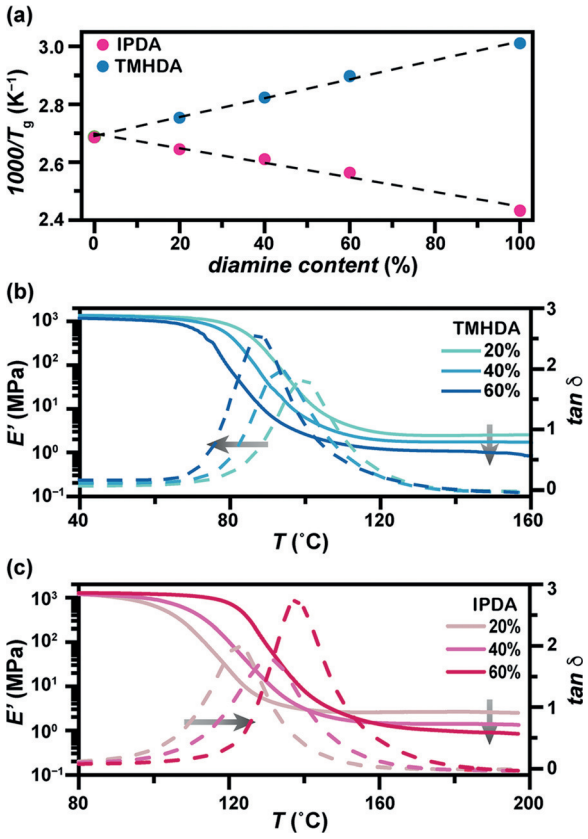

Figure 2. a) Flory–Fox analysis of PDK vitrimers **1**–**7** and linear polymers derived from TK-10 and either TMHDA or IPDA. b),c) Temperature-dependent storage modulus (E') and tanδ for TMHDA-based PDK vitrimers **2**–**4** (b), and IPDA-based vitrimers **5**–**7** (c).

material, which is available by microbial fermentation, suggesting bio-sourced feedstocks for recyclable PDK vitrimers with controlled properties are in reach.[24–26]

To synthesize this family of PDK vitrimers, where PDKs **2**–**4** incorporate 20, 40, and 60 mol% TMHDA, and PDKs **5**–**7** incorporate 20, 40, and 60 mol% IPDA (Figure 1c), the linear segments for diamine-modified PDK vitrimers were initially synthesized in the melt from ditopic triketone TK-10 and either of the diamines prior to introducing TREN to crosslink the networks. This ensured that the gel fractions were in excess of 95% to the differentiated reactivity (that is, sterics) of the various amines in the monomer feed (Supporting Information, Table S1). We did not advance to higher diamine content than 60%, as we would have eventually hit the limit for the gel point in polymer networks for mixtures of ditopic and tritopic amine monomers (ca. 74 mol% diamine relative to triamine for a 10% total amine excess relative to triketones from ditopic TK-10).

Homogeneous distribution of TMHDA and IPDA diamines in PDKs **2**–**7** is evidenced from the linearity of T_g^{-1} (determined by differential scanning calorimetry, DSC) as a function of the diamine content, which are related by the Flory–Fox equation (Figure 2a; Supporting Information, Figure S2);[27] PDK vitrimers incorporating only TK-10 and TREN, as well as linear PDK polymers synthesized from TK-10 and either TMHDA or IPDA and TK-10, provided the end-points for the comprehensive analysis. Notably, the incorporation of flexible TMHDA-based linear segments decreased T_g relative to the parent PDK network incorporating only TREN, while the incorporation of stiff IPDA-derived linear segments increased T_g; each dependency manifested in a well-behaved manner, albeit divergent. Accordingly, the predictability with which one may tune T_g in PDKs is advantageous over other network polymers where chemical heterogeneity is unavoidable, as is the case with many conventional thermosets and some thermally reprocessable thermosets based on other vitrimer chemistries. On account of their homogeneity, it also becomes possible to directly tie their emergent thermomechanical behaviors to well-defined vitrimer architectures.

To characterize the range of embodied architectural attributes of TMHDA- and IPDA-modified PDK networks, we carried out extensive dynamic mechanical analyses (DMA; Figure 2; Supporting Information, Tables S2–S4), which indicated ambient temperature storage moduli of $E' = 1.4$–2.0 GPa (Figure 2b,c) as well as tensile strengths of $\sigma = 18.5$–30 MPa (Supporting Information, Table S4), which are similar to many epoxies.[28] Furthermore, once heated above their T_g, the storage modulus of each PDK in the rubbery plateau was then used to estimate PDK crosslinking density (ν), and in turn the MW of diamine-derived linear segments between TREN-derived cross-linking points (Supporting Information, Table S2): here, such segments varied 3.8–9.6 kg mol^{-1} for THMDA loadings of 20–60%; similarly, 4.0–11.0 kg mol^{-1} for IPDA loadings of 20–60%. These data

also provided independent determination of T_g (from the maximum in tan δ) and in turn provided support for our hypothesis that the softening temperature in vitrimers is not only dictated by the MW of the polymer chains between crosslinks, but also the conformational degrees of freedom available to those chains in the network.

The rheological properties of PDK vitrimers underlie their prospects for both polymer processing during manufacturing, their mechanical response to deformation, their ageing mechanisms while in service, and their prospects for scrap recovery via remolding and reuse (namely, post-industrial recycling); we provide detailed examples of the efficacy of post-industrial PDK recycling in the Supporting Information, Figure S3). To begin unpacking the differentiated rheological characteristics of experiments whereby a strain of 1 % (within the linear viscoelastic regime) was applied to compression-molded PDK samples; the ensuing stress decay was then monitored as a function of time. As is typical for vitrimers, complete relaxation was observed after the application of strain over the entire temperature range owing to diketoenamine bond-exchange reactions. The characteristic stress-relaxation time (τ^*) is determined at ratio of e^{-1} with regard to the relaxation modulus (G) relative to the initial (G_0). We found that increasing the diamine content in PDK vitrimers resulted shorter τ^* values: for example, at $T = 150\,°C$, τ^* decreased from 151 s to 81 s with an increase in the TMHDA content from 20 % to 60 %. Since higher diamine-content vitrimers have lower moduli at the rubbery plateau, PDKs yield lower viscosity at the same temperature, that is, the active chain ends can redistribute more freely in the network. However, we also observed by comparing TMHDA- and IPDA-based vitrimers having the same diamine content (for example, 40 %) at the same temperature (for example, $T = 150\,°C$) that τ* was considerably shorter for PDK networks with higher conformational entropy: for example, $\tau^* = 110$ s for TMHDA-based PDK 3 with 6.3 kg mol^{-1} linear segments, compared to $\tau^* = 457$ s for PDK 6 with 7.8 kg mol^{-1} linear segments. IPDA-based PDKs consistently yield lower viscosity than TMHDA-based vitrimers for an equivalent diamine loading when interrogated at the same temperature, that is, the active chain ends in IPDA-based vitrimers do not redistribute as freely in the network as do those in TMHDA-based vitrimers. This confirms our hypothesis that conformational entropy dictates the rheological behavior of PDK vitrimers for a given MW of linear segments in the network (Figure 3 a,b; Supporting Information, Figures S4).

While we were able to glean key differences in the dynamic behavior associated with stress relaxation for PDK networks incorporating flexible and stiff linear segments, we were further able to assess the impact of these polymer network architectures on the activation barriers to diketoenamine bond exchange in the solid state. Here, Arrhenius behavior governs the rheological properties of PDK networks, as viscoelastic flow requires a series of bond exchange events for the network to return to equilibrium after the application of strain. For TMHDA loadings of 20–60 %, we observed E_a values of 47 ± 1.3, 46 ± 4.4, and 43 ± 1.5 kJ mol^{-1}; for IPDA loadings of 20–60 % we observed E_a values of 54 ± 4.1, 60 ± 4.3, and 62 ± 4.4 kJ mol^{-1}.

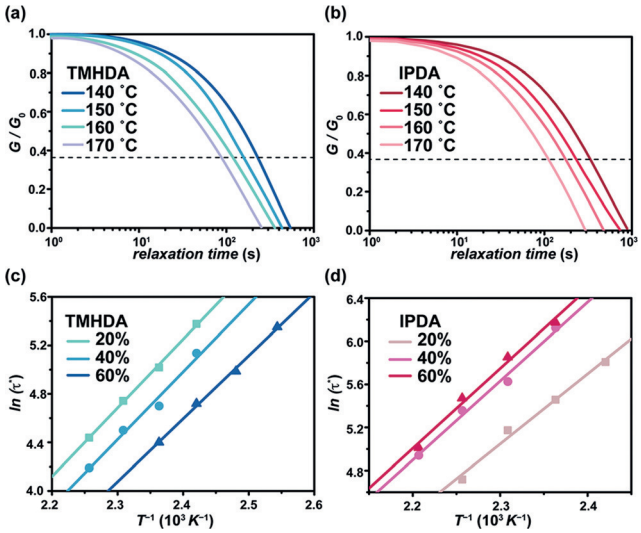

Figure 3. Normalized stress–relaxation curves at different temperatures for a) PDK **2** (20% TMHDA) and b) PDK **5** (20% IPDA). Dashed lines indicate 37% of G_0. Data were acquired at 1% strain. c),d) Arrhenius plots relating τ_0 to T^{-1} for PDKs **2**–**7**.

In general, E_a values reflect a convolution of: 1) stereoelectronics associated with the different types of amine exchange reactions that can proceed with the available electrophiles, and 2) entropic penalties associated with deforming chains, particularly when they are stiff, as is the case for IPDA-derived linear segments. To begin disentangling these contributions, we note that introducing TMHDA- and IPDA-based linear segments to the PDK network yield structurally differentiated diketoenamine bonds. As analogues to these, we synthesized *N*-neopentyl and *N*-cyclohexyl diketoenamines from 2-acetyl-5,5-dimethyl-1,3-cyclohexanedione and either neopentylamine or cyclohexylamine. To form a new crosslink in the network-in the dilute limit (that is, at high diamine loading in the PDK network)-an aminoethyl group on a di-substituted TREN would need to exchange with one of the bonds in any of the linear segments bound to the network on both chain ends. This can be evaluated by using *N*,*N*-dimethylaminoethylamine as a TREN analogue in bond exchange reactions with either the *N*-neopentyl or *N*-cyclohexyl diketoenamine small molecules (Supporting Information, Scheme S1).

After measuring the pseudo-first order bond exchange rates at various temperatures for each compound (Supporting Information, Figures S6–S8 and Table S5), we found that the activation barrier for diketoenamine bond exchange in the solid-state for TMHDA-based PDK networks at high TMHDA loading ($E_a = 43 \pm 1.5$ kJ mol^{-1}) converges to that determined for the *N*-neopentyl TMHDA-like model compound in solution ($E_a = 41 \pm 2.3$ kJ mol^{-1}). Thus, for flexible networks with increasingly lower crosslinking density, the activation barrier to bond exchange approaches that for the bond itself; it is not appreciably affected by the conformational degrees of freedom of the network, as the polymer chain to which the nucleophilic amine is appended freely explores a large number of configurations and conformations, many of which allow addition–elimination bond exchange

reactions to proceed. Most intriguingly, however, we find that solid-state activation barriers for bond exchange in IPDA networks with increasing IPDA ($E_a = 62 \pm 4.4$ kJ mol^{-1}) content diverge considerably more from that measured in solution for *N*-cyclohexyl model IPDA compound ($E_a = 48 \pm 0.12$ kJ mol^{-1}), by as much as 14 kJ mol^{-1}. This reflects the added influence of stiffness and conformational entropy, which significantly reduces the number of states available for exocyclic hemiaminal loop formation, which underlies diketoenamine bond exchange.

Thus, while there has been extensive effort to understand differences in E_a for bond exchange reactions for small molecule vitrimer analogues in solution and for fully formed vitrimers in the solid-state, only now have we discerned that for architecturally similar vitrimers, microstructural differences in the monomer constituents play the dominant role in the observed materials properties, both in and out of equilibrium. Moreover, this dynamic behavior appears to be controllable at the level of monomers, as these choices set forth the energy landscapes available to the system to reconfigure. Related effects tied to conformational entropy have been seen in loop formation elsewhere, for example in multivalent and intramolecular ligand–receptor interactions.[29–32]

We further evaluated the impact of network microstructure on how PDK vitrimers flow for architecturally similar networks by determining, via the Maxwell relation, the topology freezing transition temperature (T_v), which relates the temperature at which the vitrimer's viscosity increases above $\eta = 10^{12}$ Pa s. For all PDK vitrimers, $T_v < T_g$, indicating that the topology of network remains frozen below T_g even though bond exchange reactions are, in principle, allowed. It is further notable that T_v decreased from −20 °C to −45 °C as the TMHDA loading was increased from 20 % to 60 %, whereas it increased from −1 °C to 11 °C as the IPDA loading was increased from 20 % to 60 % (Supporting Information, Table S3). This indicates that the softer TMHDA-derived linear segments allow the network to flow more easily, while the more rigid IPDA-derived linear segments make flow more difficult.

Toward a molecular understanding of how TMHDA and IPDA exert their distinctive influence on the rheological properties of PDKs, we computationally explored the conformational degrees of freedom of each species by scanning the torsional potential of bonds involved, which are highly differentiated in their flexibilities. We also computed the corresponding torsional partition functions q_{tor}. The torsional potential scans were performed by rotating a bond 360 degrees and allowing the remainder of the molecule to relax. Conformation searches were performed to obtain the global minimum energy conformations to be used as starting points, and further conformation searches were carried out at intermediate steps of the scans to ensure full relaxation of the molecule outside of the bond involved in the scan (see the Supporting Information). The torsional potential of all of the rotating bonds for TMHDA and IPDA were examined: bonds B1–7 and bonds B1–3, respectively (Figure 4, insets). The partition functions q_{tor} provide a sense of the number of states thermally accessible to each species by torsional rotation.

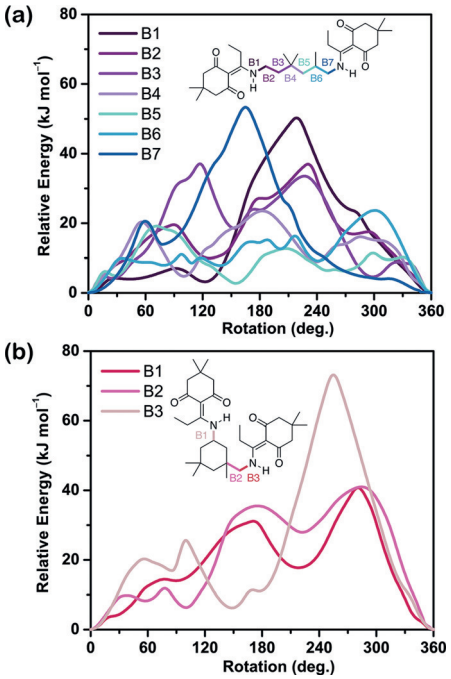

Figure 4. Torsional strain energies for various bonds in model compounds representing a) TMHDA-based and b) IPDA-based PDK monomer segments.

These quantities for TMHDA- and IPDA-based monomer segments are presented in Figure 1 b, and their ratio in the Supporting Information, Figure S6. Segments based on TMHDA possess a greater number of accessible states up to 10 $k_B T$. This difference in accessible states is related, in part, to the difference in the number of rotatable bonds, but also the energy landscapes for bond rotation, which are chemistry-specific. For example, strictly considering the number of bonds rather than the chemistry of each monomer segment, a ratio of 7:3 (ca. 2.33) would be expected. However, the calculations show q(THMDA)/q(IPDA) values are higher across the range of $k_B T$, highlighting the critical role of each monomer segment's embodied chemistry. This ratio reaches a maximum of 3.33 near 2 $k_B T$, and decreases at higher $k_B T$ as more of the conformational states become accessible to the IPDA segments (Supporting Information, Figure S9). This fundamental difference in flexibility gives rise to the differences observed rheological properties at elevated temperature of PDKs that incorporate microstructural elements with varying conformational entropy.

Microstructural and architectural attributes of PDK vitrimers (and likely others) therefore emerge as powerful elements of design for controlling the thermomechanical behavior of vitrimers in and out of equilibrium, with respect to the bond exchange reactions foundational to their reconfigurability and the conformational entropy of polymer chains in the network. Entropic and stereoelectronic considerations can result in divergent energetics to bond exchange in the solid state by as much as 19 kJ mol^{-1} for architecturally similar networks incorporating chains with varying conformational degrees of freedom, or structure of nucleophilic amine and electrophilic diketoenamine partners. We further see

controllably divergent dependencies for both T_g and T_v with flexible and stiff diamine monomers, highlighting the distinctive role played by microstructure on these characteristics. Their influence on vitrimer dynamics cannot be understated and suggest exciting paths forward for controlling vitrimer processing.

Acknowledgements

The technical scope of work was supported by the Laboratory Directed Research and Development Program of Lawrence Berkeley National Laboratory under U.S. Department of Energy Contract No. DE-AC02-05CH11231. Portions of this work, including organic and polymer synthesis and characterization, were carried out as a User Project at the Molecular Foundry, which is supported by the Office of Science, Office of Basic Energy Sciences, of the U.S. Department of Energy under the same contract. Computational resources were provided by the Savio cluster of the Berkeley Research Computing program at the University of California, Berkeley. The computational effort was partially supported by the Joint Center for Energy Storage Research (JCESR), an Energy Innovation Hub funded by the U.S. Department of Energy, Office of Science, Office of Basic Energy Sciences (BES). R.K.W. was supported by the US Department of Energy, Office of Science, Office of Workforce Development for Teachers and Scientists (WDTS) under the Science Undergraduate Laboratory Internship (SULI) program.

Conflict of interest

The authors declare the following competing interests: B.A.H. and P.R.C. are inventors on US provisional patent application 62/587,148 submitted by Lawrence Berkeley National Laboratory that covers poly(diketoenamine)s, as well as aspects of their use and recovery.

Keywords: conformational entropy · mechanical properties · poly(diketoenamine) · rheology · vitrimers

How to cite: *Angew. Chem. Int. Ed.* **2020**, *59*, 735–739
Angew. Chem. **2020**, *132*, 745–749

[1] D. Montarnal, M. Capelot, F. Tournilhac, L. Leibler, *Science* **2011**, *334*, 965–968.
[2] W. Denissen, J. M. Winne, F. E. Du Prez, *Chem. Sci.* **2016**, *7*, 30–38.
[3] D. J. Fortman, J. P. Brutman, G. X. De Hoe, R. L. Snyder, W. R. Dichtel, M. A. Hillmyer, *ACS Sustainable Chem. Eng.* **2018**, *6*, 11145–11159.
[4] J. Brutman, A. Delgado, M. A. Hillmyer, *ACS Macro Lett.* **2014**, *3*, 607–610.
[5] Y. Zhou, J. P. Goossens, R. Sijbesma, J. A. Heuts, *Macromolecules* **2017**, *50*, 6742–6751.
[6] J. Han, T. Liu, C. Hao, S. Zhang, B. Guo, J. Zhang, *Macromolecules* **2018**, *51*, 6789–6799.
[7] D. J. Fortman, J. P. Brutman, C. J. Cramer, M. A. Hillmyer, W. R. Dichtel, *J. Am. Chem. Soc.* **2015**, *137*, 14019–14022.
[8] N. Zheng, J. Hou, Y. Xu, Z. Fang, W. Zou, Q. Zhao, T. Xie, *ACS Macro Lett.* **2017**, *6*, 326–330.
[9] N. Zheng, Z. Fang, W. Zou, Q. Zhao, T. Xie, *Angew. Chem. Int. Ed.* **2016**, *55*, 11421–11425; *Angew. Chem.* **2016**, *128*, 11593–11597.
[10] X. Chen, L. Li, K. Jin, J. Torkelson, *Polym. Chem.* **2017**, *8*, 6349–6355.
[11] M. Capelot, D. Montarnal, F. Tournilhac, L. Leibler, *J. Am. Chem. Soc.* **2012**, *134*, 7664–7667.
[12] M. Röttger, T. Domenech, R. van der Weegen, A. Breuillac, R. Nicolay, L. Leibler, *Science* **2017**, *356*, 62–65.
[13] W. Ogden, Z. Guan, *J. Am. Chem. Soc.* **2018**, *140*, 6217–6220.
[14] O. R. Cromwell, J. Chung, Z. Guan, *J. Am. Chem. Soc.* **2015**, *137*, 6492–6495.
[15] P. Zheng, T. J. McCarthy, *J. Am. Chem. Soc.* **2012**, *134*, 2024–2027.
[16] Y. Nishimura, J. Chung, H. Muradyan, Z. Guan, *J. Am. Chem. Soc.* **2017**, *139*, 14881–14884.
[17] M. M. Obadia, B. P. Mudraboyina, A. Serghei, D. Montarnal, E. Drockenmuller, *J. Am. Chem. Soc.* **2015**, *137*, 6078–6083.
[18] P. Taynton, K. Yu, R. K. Shoemaker, Y. Jin, H. J. Qi, W. Zhang, *Adv. Mater.* **2014**, *26*, 3938–3942.
[19] P. Taynton, H. Ni, C. Zhu, K. Yu, S. Loob, Y. Jin, H. J. Qi, W. Zhang, *Adv. Mater.* **2016**, *49*, 6277–6284.
[20] W. Denissen, G. Rivero, R. Nicolaÿ, L. Leibler, J. M. Winne, F. E. Du Prez, *Adv. Funct. Mater.* **2015**, *25*, 2451–2457.
[21] W. Denissen, M. Droesbeke, R. Nicolay, L. Leibler, J. M. Winne, F. E. Du Prez, *Nat. Commun.* **2017**, *8*, 14857.
[22] J. J. Lessard, L. F. Garcia, C. P. Easterling, M. B. Sims, K. C. Bentz, S. Arencibia, D. A. Savin, B. S. Sumerlin, *Macromolecules* **2019**, *52*, 2105–2111.
[23] P. R. Christensen, A. M. Scheuermann, K. E. Loeffler, B. A. Helms, *Nat. Chem.* **2019**, *11*, 442–448.
[24] V. Froidevaux, C. Negrell, S. Caillol, J. P. Pascault, B. Boutevin, *Chem. Rev.* **2016**, *116*, 14181–14224.
[25] R. L. Shriner, H. R. Todd, *Org. Synth.* **1935**, *15*, 14–16.
[26] P. Anbarasan, Z. C. Baer, S. Sreekumar, E. Gross, J. B. Binder, H. W. Blanch, D. S. Clark, F. D. Toste, *Nature* **2012**, *491*, 235–239.
[27] T. G. Fox, Jr., P. J. Flory, *J. Appl. Phys.* **1950**, *21*, 581–591.
[28] R. Auvergne, S. Caillol, G. David, B. Boutevin, J.-P. Pascault, *Chem. Rev.* **2014**, *114*, 1082–1115.
[29] V. M. Krishnamurthy, V. Semetey, P. J. Bracher, N. Shen, G. M. Whitesides, *J. Am. Chem. Soc.* **2007**, *129*, 1312–1320.
[30] H. Adams, E. Chekmeneva, C. A. Hunter, M. C. Misuraca, C. Navarro, S. M. Turega, *J. Am. Chem. Soc.* **2013**, *135*, 1853–1863.
[31] E. Papaleo, G. Saladino, M. Lambrughi, K. Lindorff-Larsen, F. L. Gervasio, R. Nussinov, *Chem. Rev.* **2016**, *116*, 6391–6423.
[32] D. Mariottini, A. Idili, M. A. D. Nijenhuis, T. F. A. de Greef, F. Ricci, *J. Am. Chem. Soc.* **2018**, *140*, 14725–14734.

Manuscript received: September 24, 2019
Accepted manuscript online: October 15, 2019
Version of record online: November 21, 2019

